



ELSEVIER

15 February 1999

PHYSICS LETTERS A

Physics Letters A 252 (1999) 20–26

## Nonlinear signal amplification in a 2D system operating in static and oscillatory regimes

M.E. Inchiosa<sup>a,1</sup>, A.R. Bulsara<sup>a,2</sup>, K.A. Wiesenfeld<sup>b,3</sup>, L. Gammaitoni<sup>c,d,4</sup><sup>a</sup> *Space and Naval Warfare Systems Center, San Diego, Code D364, San Diego, CA 92152-5001, USA*<sup>b</sup> *School of Physics, Georgia Institute of Technology, Atlanta, GA 30332, USA*<sup>c</sup> *Dipartimento di Fisica, Università di Perugia, I-06100 Perugia, Italy*<sup>d</sup> *Istituto Nazionale de Fisica Nucleare, I-06100 Perugia, Italy*

Received 18 November 1998; accepted for publication 1 December 1998

Communicated by C.R. Doering

### Abstract

We study the spectral response of a nonlinear system of coupled oscillator equations representing the overdamped two-junction (dc) superconducting quantum interference device (SQUID) loop; this system admits of static or oscillatory solutions for the autonomous case. In the presence of a weak time-dependent sinusoidal target signal and noise we find, in the regime of oscillatory or “running” solutions, an enhancement of the response (characterized by an output signal-to-noise ratio at the drive frequency) as a function of the intrinsic device parameters as well as *externally controlled* bias parameters that determine the nature of the long-time solutions. Modeling the device via a derived input–output transfer characteristic yields results in good agreement with recent experiments. This work offers a technique whereby the response of nonlinear devices with similar response characteristics may be optimized without directly adjusting the system noise. © 1999 Published by Elsevier Science B.V.

PACS: 05.40.+j; 02.50.Ey; 02.30.Hq; 85.25.Dq

Periodically modulated nonlinear stochastic systems have received considerable attention lately, exhibiting a richness of noise-mediated resonance behavior in the response. Recent experiments and calculations have explored variants of one such effect, stochastic resonance (SR) (for good overviews see Ref. [1]), in a single-junction (rf) superconducting quantum interference device (SQUID) loop [2–4]. In this Letter, we offer a theoretical description of some

intriguing behavior seen in recent experiments [5] involving a two-junction (dc) SQUID operated as a nonlinear dynamic detector of very weak time-sinusoidal magnetic signals. The observed behavior can be *externally* controlled by adjusting an applied dc magnetic flux and bias current, without directly adjusting the device noise, in contrast to SR scenarios. This additional freedom of control is quite valuable, since it allows significantly higher output power and signal-to-noise ratio (SNR).

The rf SQUID has a potential energy function that changes from multistable to monostable as bias parameters are adjusted, but the dc SQUID’s potential

<sup>1</sup> E-mail: inchiosa@spawar.navy.mil.<sup>2</sup> E-mail: bulsara@spawar.navy.mil.<sup>3</sup> E-mail: kw2@prism.gatech.edu.<sup>4</sup> E-mail: gammaitoni@perugia.infn.it.

energy function changes from multistable to *unstable*. Specifically, the dc SQUID is an example of a dynamic system that is characterized by a (in this case, 2D) potential energy function and admits of one or more static solutions corresponding to minima of the potential, as well as oscillatory or “running” solutions when the bias conditions remove the potential minima. When the potential has minima the output flux characteristic is hysteretic and the long-time solutions of the dynamics (in the absence of the sinusoidal driving term) are static, not oscillatory. When the bias conditions remove the potential minima, the time-averaged output flux characteristic becomes non-hysteretic, and for our purposes the signal processing properties of the dc SQUID become describable via a static, nonlinear input–output function or “transfer characteristic” (TC).

In the SR effect [1] the output power or output SNR, measured at the frequency of a small sinusoidal target signal, passes through a maximum as a function of the input or device noise power; the critical noise intensity at the maximum can be related to a matching of deterministic and stochastic time scales. In contrast to such an SR scenario, here we study the maximization of the output SNR as a function of (experimentally controllable) dc bias parameters. Adjusting the bias parameters to move out of the hysteretic regime and into the regime of running solutions greatly increases output power and SNR. The maximization, obtained for a fixed input SNR and without directly adjusting the system noise, is independent of any time scale matching and is not SR. We note that, in the signal detection context, alternate (to the output SNR) measures of performance involving an information-theoretic characterization of the system response, have been proposed recently [6]; these measures take into account the entire probabilistic structure of the response and permit one to characterize the response to aperiodic signals, when the output SNR can become ill-defined.

The dc SQUID consists of two Josephson junctions inserted into a superconducting loop [7]; we assume, for convenience, that the insertion is symmetric. When used as a magnetometer, the dc SQUID’s “input” is an externally applied magnetic flux  $\Phi_e$ . Conventionally, the voltage measured across the Josephson junctions is taken as its “output”. Instead, we take the circulating current  $I_s$  (experimentally measured via the associated

“shielding flux”) as output. This setup was developed for studying SR in dc SQUIDs operating in a hysteretic regime. However, much higher output signal strengths and SNRs were discovered by using dc bias currents large enough to take the device beyond the hysteretic regime into the regime of running solutions. These higher input–output gains result from the rapid change of  $I_s$  with  $\Phi_e$  where the dynamics change from static to oscillatory. In what follows, we first derive the TC from dynamical equations describing the dc SQUID. We then go on to compute the output SNR at the frequency of an applied sinusoidal signal.

An external magnetic field produces a geometrical flux  $\Phi_e$  inside the loop; in turn, the flux quantization condition [7] leads to an induced circulating (or shielding) current  $I_s$  that screens the applied flux so that the total loop flux may be cast in the form

$$\Phi = \Phi_e + LI_s, \quad (1)$$

$L$  being the loop inductance. Further, the single-valuedness of the wave function around the loop leads to the phase continuity condition

$$\delta_2 - \delta_1 = 2\pi n - 2\pi\Phi/\Phi_0, \quad (2)$$

$n$  being an integer, and  $\Phi_0 \equiv h/2e$  being the flux quantum. Taking  $n = 0$ , we obtain

$$\beta \frac{I_s}{I_0} = \delta_1 - \delta_2 - 2\pi \frac{\Phi_e}{\Phi_0}, \quad (3)$$

where  $I_0$  is the critical current of the junctions (assumed identical) and  $\beta \equiv 2\pi LI_0/\Phi_0$  is the nonlinearity parameter. In the absence of noise and the target magnetic flux (taken to be sinusoidal in this work), we can use the RSJ model to write down equations for the currents in the two arms of the SQUID via a lumped circuit representation [7]; expressed via the Josephson relations  $\dot{\delta}_i = 2eV_i/\hbar$  linking the voltage and the quantum phase difference across the junction  $i$ , these equations take the form

$$\begin{aligned} \tau \dot{\delta}_1 &= \frac{1}{2}I_b - I_s - I_0 \sin \delta_1, \\ \tau \dot{\delta}_2 &= \frac{1}{2}I_b + I_s - I_0 \sin \delta_2, \end{aligned} \quad (4)$$

where  $\tau \equiv \frac{1}{2}\hbar Re$ ,  $R$  being the normal state resistance of the junctions. The dc bias current  $I_b$  is applied symmetrically to the loop. In experiments [5], the bias current and applied flux are externally controllable.

Eqs. (4) can be rewritten in terms of the gradient of a two-dimensional potential energy function as  $\dot{\delta}_i = \partial U / \partial \delta_i$ , with the time rescaled by  $\tau$ , and the potential function defined as

$$U(\delta_1, \delta_2) = -\cos \delta_1 - \cos \delta_2 - J(\delta_1 + \delta_2) + (2\beta)^{-1}(\delta_1 - \delta_2 - 2\pi\Phi_{\text{ex}})^2, \quad (5)$$

where we introduce the dimensionless bias current  $J \equiv I_b / 2I_0$  and applied flux  $\Phi_{\text{ex}} \equiv \Phi_c / \Phi_0$ . Two distinct regimes of operation, corresponding to superconducting and running states, are possible.

When the potential (5) has minima, the SQUID is superconducting. The symmetry of the potential and the energy barrier height between stable states can be controlled, respectively, by adjusting the parameters  $\Phi_{\text{ex}}$  and  $J$ . This configuration (including the problem of thermal activation out of the stable states of the potential) has been discussed in the literature [8]. After a brief transient, the phase angles  $\delta_{1,2}$  achieve constant steady-state values and one obtains the conditions for the minima via  $\dot{\delta}_{1,2} = 0$ . This leads to the current equations:

$$\begin{aligned} I_b &= I_0(\sin \delta_1 + \sin \delta_2), \\ 2I_s &= I_0(\sin \delta_2 - \sin \delta_1), \end{aligned} \quad (6)$$

whence, using the continuity condition (2), the circulating current may be cast in the form  $I_s / I_0 = -\cos \frac{1}{2}(\delta_1 + \delta_2) \sin \pi(\Phi / \Phi_0)$ . Noting (from (6)) that  $\sin \delta_2 = J + I_s / I_0$ , and using (2) again, we may write down the following transcendental equation for the circulating current in the superconducting regime:

$$\begin{aligned} \frac{I_s}{I_0} &= -\sin \left( \pi\Phi_{\text{ex}} + \frac{\beta I_s}{2I_0} \right) \\ &\times \cos \left[ \sin^{-1} \left( J + \frac{I_s}{I_0} \right) + \pi\Phi_{\text{ex}} + \frac{\beta I_s}{2I_0} \right]. \end{aligned} \quad (7)$$

Eq. (7) may be solved numerically for the circulating current; the ensuing TC is periodic in the applied flux  $\Phi_{\text{ex}}$  and possibly hysteretic, with the hysteresis loop width controlled by the bias current  $J$ . For  $J = 0$  one obtains hysteresis for any nonlinearity  $\beta$ ; for  $0 < J \leq 1$ , hysteresis occurs over some range of  $\beta$ .

Assume  $J$  is large enough to put the SQUID in the nonhysteretic regime. Let  $\Phi_{\text{ex}1}$  be the critical flux at which, as  $\Phi_{\text{ex}}$  is increased from 0 to  $\frac{1}{2}$ , the potential's minima disappear and running solutions replace

static ones. For  $\Phi_{\text{ex}}$  increasing from  $\frac{1}{2}$  to 1, running solutions disappear at  $\Phi_{\text{ex}2} \equiv 1 - \Phi_{\text{ex}1}$ . The quantities  $\Phi_{\text{ex}1}, \Phi_{\text{ex}2}$  will aid us in determining the TC and, later, the output SNR. At  $\Phi_{\text{ex}} = \Phi_{\text{ex}1,2}$ , the function  $f = \sin \delta_1 + \sin \delta_2 - 2J$  will have a maximum that coincides with  $f = 0$ ; i.e., a plot of  $f$  versus  $\delta_1$  (with  $\delta_2$  given by the continuity condition) touches the  $\delta_1$  axis from below. To determine the location of this maximum one maximizes  $f$ , subject to the continuity condition; i.e., one constructs the function  $g = f + \lambda(\delta_2 - \delta_1 - \beta \sin \delta_1 + \beta J + 2\pi\Phi_{\text{ex}})$ , and eliminates the Lagrange multiplier  $\lambda$  while solving for  $\delta_{1c}$  via the conditions  $\partial g / \partial \delta_{1,2} = 0$ . Finally we obtain

$$\begin{aligned} \sin \delta_{1c} &= 2J - \sqrt{1 - \left( \frac{\cos \delta_{1c}}{1 + \beta \cos \delta_{1c}} \right)^2}, \\ \cos \delta_{2c} &= -\frac{\cos \delta_{1c}}{1 + \beta \cos \delta_{1c}}. \end{aligned} \quad (8)$$

By selecting the appropriate solution of (8) and using (3), (6), and the continuity condition, one obtains  $\Phi_{\text{ex}2}$  (up to an integer constant). In the interval  $\Phi_{\text{ex}1} \leq \Phi_{\text{ex}} \leq \Phi_{\text{ex}2}$ , the solutions to the dynamic equations (4) are oscillatory at long times. The oscillation period tends to infinity very close to  $\Phi_{\text{ex}1}$ , decreases as  $\Phi_{\text{ex}} \rightarrow \frac{1}{2}$ , and increases again as  $\Phi_{\text{ex}} \rightarrow \Phi_{\text{ex}2}$ . The interval  $(\Phi_{\text{ex}1}, \Phi_{\text{ex}2})$  of the running solutions increases with  $J$ . Note that an approximate solution to the system (8) can be constructed by assuming (for large  $\beta$ ) a zero-order solution  $\delta_{10} \approx \sin^{-1}(2J - 1)$ , whence one obtains to first order  $\delta_{1c} \approx \delta_{10} - h(\delta_{10}) / h'(\delta_{10})$ , with the identification  $h(\delta_{1c}) \equiv 2J - \sin \delta_{1c} - \{1 - [\cos \delta_{1c} / (1 + \beta \cos \delta_{1c})]^2\}^{1/2}$  and the prime denoting differentiation with respect to  $\delta_{1c}$ .

Fig. 1 shows  $\Phi_{\text{ex}1}$  versus the circulating current  $J$  for different  $\beta$ . The solid curves are obtained via numerical solution of the system (8), while the dashed curves represent the perturbation approximation outlined above. As expected, the approximation works best at large  $\beta$ ; with decreasing  $\beta$ , it works best at the higher  $J$  values. For a given  $\beta$ , the critical  $J$  at which the running solutions first develop corresponds to  $\Phi_{\text{ex}1} = \frac{1}{2}$ .

The running solutions regime has been investigated [9] mainly via a computation of the voltage across the Josephson junctions; however, our present considerations require us to consider the circulating current instead. Fig. 2 shows a sequence of TCs ob-

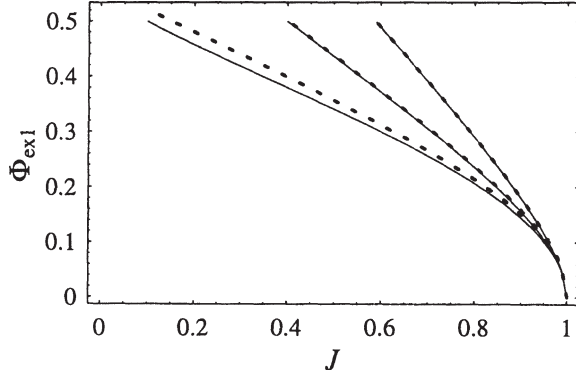


Fig. 1. Critical applied flux  $\Phi_{\text{ex1}}$  versus dc bias current  $J$  for  $\beta = 0.4, 2.0, 4.0$  (reading from left-to-right). Solid curves: numerical solution via (8); dashed curve: theoretical approximation (see text).

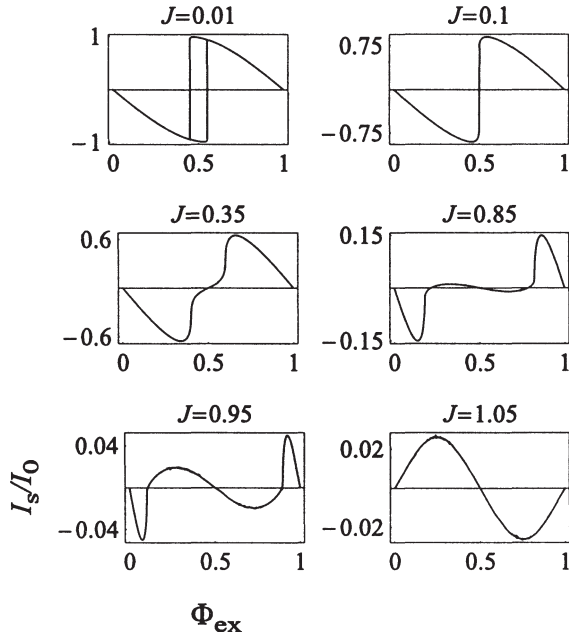


Fig. 2. Transfer characteristic: time-averaged circulating current (see text)  $I_s/I_0$  versus applied flux  $\Phi_{\text{ex}}$  for  $\beta = 0.4$ .

tained via numerical solution of (4); they show good agreement with the experimentally obtained TCs [5]. The TC is periodic in  $\Phi_{\text{ex}}$  with only one complete  $\Phi_{\text{ex}}$  cycle shown for each  $J$ . In the static solutions regime, the TC is exactly reproducible by solving the transcendental equation (7). The demise of hysteresis for increasing  $J$  is clearly evident. In the running regime, the average circulating current is obtained from the

solution of (4) by performing a time-average over the period of oscillations in  $\delta_{1,2}(t)$ ; in experiments [5], this is the measured quantity since the oscillation frequency is very high. The TCs are symmetric about  $\Phi_{\text{ex}} = \frac{1}{2}$ , at which point the average circulating current vanishes. Interestingly, we observe a small “ripple” (centered on  $\Phi_{\text{ex}} = \frac{1}{2}$ ) almost spanning the regime of the running solutions in each case. This ripple is also present in experimentally obtained TCs [5]. Note the vertical scales in Fig. 2: with increasing  $J$  the TCs decrease in range, resulting in generally less signal gain. With higher  $\beta$  (not shown), the disappearance of hysteresis and concomitant appearance of running solutions occurs at higher  $J$  values. This can be expected through examination of the potential function: larger nonlinearity  $\beta$  implies deeper wells, and a greater  $J$  is required to remove the wells (recall that  $J \leq 1$ ; for  $J > 1$ , one always gets only running solutions). Also, with higher  $\beta$ 's the “ripple” only occurs for  $J$ 's slightly less than unity, where the response is very weak; therefore, this feature may not be evident in such SQUIDs. We note, in passing, that a total flux  $\Phi$  or shielding flux  $\Phi_s \equiv LI_s$  versus  $\Phi_e$  TC can readily be computed from the  $I_s$  versus  $\Phi_e$  TC.

An analytic approximation to the TC for the case of small  $\beta$  captures most of the interesting behavior for  $J < 1$ . In this regime, one can obtain an approximate solution in the running state by introducing the sum and difference variables  $\delta = \frac{1}{2}(\delta_1 - \delta_2)$ ,  $\Sigma = \frac{1}{2}(\delta_1 + \delta_2)$ , which obey the equations

$$\begin{aligned} \dot{\delta} &= -2\beta^{-1}(\delta - \frac{1}{2}\pi\Phi_{\text{ex}}) - \cos \Sigma \sin \delta, \\ \dot{\Sigma} &= J - \cos \delta \sin \Sigma \end{aligned} \quad (9)$$

(with the time rescaled by  $\tau$ ), and then realizing that  $\delta = \frac{1}{2}\pi\Phi_{\text{ex}}$  is an approximate solution of the  $\delta$  equation for very small  $\beta$ . Substituting this solution into the  $\Sigma$  equation, we may perform the integration to obtain

$$\begin{aligned} \Sigma(t) &= 2 \tan^{-1} \left\{ \frac{\Omega}{J} \tan \left[ \frac{1}{2} \Omega t - \tan^{-1} \left( \frac{\cos \pi \Phi_{\text{ex}}}{\Omega} \right) \right] \right. \\ &\quad \left. + \frac{\cos \pi \Phi_{\text{ex}}}{J} \right\}, \end{aligned} \quad (10)$$

where  $\Omega \equiv (J^2 - \cos^2 \pi \Phi_{\text{ex}})^{1/2}$ . At  $\Phi_{\text{ex}} = \frac{1}{2}$ , the above expression reduces to  $\Sigma = Jt$ . A more accurate value for  $\delta$  may now be obtained by re-substituting the solution (10) into the  $\delta$  equation. The solution (obtained numerically) may be used to compute the TC

via (3), following the above-described time-averaging over the period of the running solutions. The resulting TC is qualitatively similar to the one obtained via direct numerical solution of (4) in the running solutions regime, with the agreement improving as  $\beta$  decreases and  $J$  increases.

Having obtained TCs, we can move on to calculating output signal power and SNR. We take the applied flux  $\Phi_{\text{ex}}$  to be the sum of a sinusoidal target input signal, colored input noise, and a dc bias flux  $\Phi_{\text{bias}}$ . The input signal power  $S$  and input noise power  $N$  (measured within a fixed frequency interval around the target signal frequency) are taken arbitrarily small, but with an input SNR  $R_{\text{in}} \equiv S/N$ ,  $10 \log_{10} R_{\text{in}} = 32$  dB (representative of values measured experimentally). Because the input signal and noise are weak, they are transformed by the device in a nearly linear manner, simply being multiplied by the slope (or “gain”  $G$ ) of the TC at the bias value  $\Phi_{\text{ex}} = \Phi_{\text{bias}}$ . (We have studied the high input amplitude, strongly nonlinear response regime in the single junction (rf) SQUID [4].) In keeping with the experimental conditions [5], we assume a smooth, band-limited input noise power spectrum, and the input signal and noise are limited to frequencies far smaller than the SQUID bandwidth ( $\tau^{-1}$ ). In the experiments, the sensing SQUID’s “output” was measured by coupling its shielding flux to a conventionally operated SQUID magnetometer via a superconducting inductive current divider network with a power coupling efficiency  $\epsilon = 0.45$ . In the experiments [5], the input noise power  $N$  comes not from an external noise generator but from the internal noise of the sensing SQUID itself. To be consistent, we introduce a “noise floor” power  $N_f = N$  to account for the internal noise in the measuring SQUID. This yields an output SNR of

$$R = \frac{SG^2\epsilon}{NG^2\epsilon + N_f} = \frac{R_{\text{in}}G^2\epsilon}{G^2\epsilon + 1}. \quad (11)$$

When the output SNR  $R$  is maximal, the gain  $G \gg 1$ , and (11) implies that  $R_{\text{in}} \approx R$ , giving us a good estimate of the input SNR from the maximal output SNR. The minimum output SNR in the theory can reach zero ( $-\infty$  dB) at the zero-slope points of the transfer characteristic. However, in the experiment the SNR will not go down to zero because of two factors: (i) the sine wave input signal does not in reality have

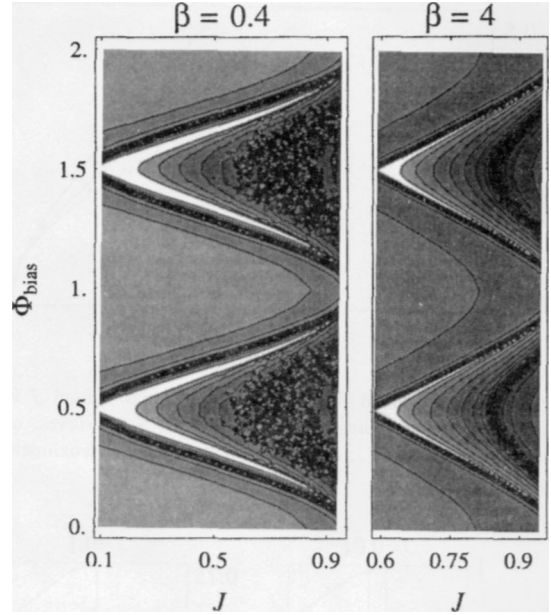


Fig. 3. Contour plot showing theoretically predicted output SNR (taken at target signal frequency), in the running solutions regime, versus bias parameters  $\Phi_{\text{bias}}$  and  $J$ . SNR scale (black-to-white) corresponds to  $-28$  dB to  $32$  dB, with contour lines spaced  $5$  dB apart (SNR values of  $-28$  dB or less are represented by black; a “speckled” appearance in the black regions of the  $\beta = 0.4$  plot is due to limited numerical precision).

infinitesimally small amplitude, and therefore samples the slope of the transfer characteristic at more than one point, and (ii) noise causes a slight fuzzing out of the transfer characteristic, so it is impossible to sit exactly on the zero slope point for an infinitely long time.

In Fig. 3 we show the output SNR versus the control parameters  $J$  and  $\Phi_{\text{bias}}$ . The  $\Phi_{\text{bias}}$  values shown cover two periods of the TC, and the SNR contour plots reflect this periodicity. The  $J$  values shown cover the range over which the dc SQUID has both static and running states (depending on the value of  $\Phi_{\text{bias}}$ ). This range is characterized by a split in the maximal SNR; one observes “bifurcating crests” separated, vertically, by  $\Phi_{\text{ex}2} - \Phi_{\text{ex}1}$ . The SNR depends on the slope of the TC: the SNR is maximal on the segments with maximum slope. The troughs running just outside the crests correspond to zero-slope points at minima and maxima of the TC. With increasing  $\beta$  the range of  $J$  values yielding both static and running solutions shrinks. Also, for large  $\beta$ ’s the crests become less evident, but the troughs remain. For  $J > 1$ , the Josephson junctions

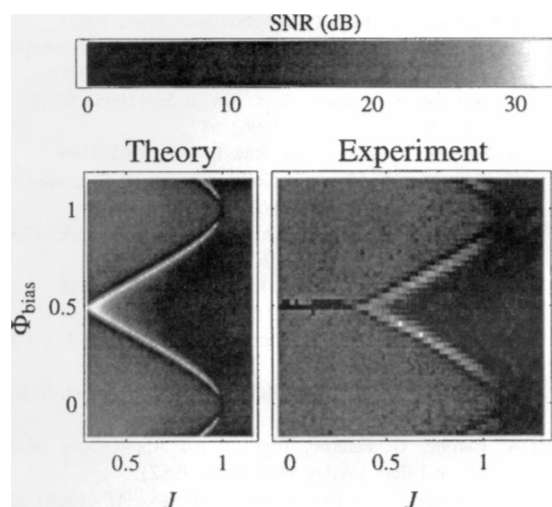


Fig. 4. Gray-scale plots of theoretically predicted and experimentally measured output SNR (taken at target signal frequency) versus bias parameters  $\Phi_{\text{bias}}$  and  $J$ . SNR scale (black-to-white) corresponds to 0 dB to 32 dB (SNR values of 0 dB or less are represented by black).  $\beta = 1.33$ .

are normal and the transfer characteristic has a much reduced range, resulting in a minimal output SNR.

As for the hysteretic regime, our earlier work on double-well potentials [3] predicts that the output at the fundamental of the applied frequency will show a maximum as a function of asymmetry (tilting of the double-well potential). Deviations from symmetry lead to a decrease of the spectral amplitude at the fundamental. This is borne out in experiments [5] which show a maximal SNR at the fundamental in a narrow band centered about  $\Phi_{\text{bias}} = \frac{1}{2}n$  ( $n$  odd), where the dc SQUID potential is symmetric. This persists up to the value of the bias current  $J$  for which hysteresis disappears (the lower limits for the horizontal axes in Fig. 3). At this point, the running solutions regime studied in the present work commences, and one obtains the “bifurcating” SNR crests and troughs. In contrast to previous work [4], we have predicted the behavior of the dc SQUID by relying directly on the dc SQUID equations.

In Fig. 4 we compare theoretical SNR predictions with experimental measurements reproduced from Ref. [5]. It is gratifying that the simple model (4) of the SQUID, together with (11), reproduces much of the complex behavior observed in the experiments. In particular, the onset of running states (the left end

of the V-shaped bifurcating crests) is consistent with theoretical predictions (cf. Fig. 1), and the shape of the bifurcating crests in the theoretical plots matches the experimental observations very well. We believe that the slight discrepancies in the positions of features relative to the  $J$  axis are due to uncertainties in the experimentally obtained value of the critical current  $I_0$ , which is used to compute the  $J$  values. Other quantitative differences between the theory and experiments may be due to the fact that the experimental SQUID is inductively coupled to a measurement or readout SQUID that is operated in the conventional “flux-locked” mode (see below), and coupling effects (if important) should be introduced into the dynamical equations (4). This is currently under investigation. We have also ignored the effects of junction capacitance, which is generally of minor significance.

SQUIDs are conventionally operated in a “flux-locked” mode [7] wherein the device is used as a null detector via a controlling feedback loop that “locks” the SQUID to an operating point on its input–output TC (usually consisting of a plot of output voltage versus input magnetic flux). Noise can cause the device to lose the null point (the slew rate problem), and establishing another stable operating point is necessary before measurements can be resumed. It has been shown, in this work as well as in experiments [5], that allowing the SQUID to operate as a free-running nonlinear dynamic device enables one to optimize its performance (for a given input SNR) by “tuning” the TC via an adjustment of externally controlled bias parameters. This is important because the nonlinearity parameter  $\beta$  cannot easily be changed after fabrication. The optimization is independent of the input SNR and does not require control of the noise.

It is important to stress that devices other than SQUIDs which nevertheless have a response characterized by TCs similar to those displayed in Fig. 2 should also show these effects. We also note that an input SNR that exceeds a threshold value can lead to an output SNR in excess of the input SNR; this situation, discussed by us in earlier work [4], is not addressed here. It is hoped that further investigations along the lines of this work, together with sophisticated arraying techniques, will lead to practical SQUIDs that are substantially more noise-tolerant than their existing counterparts.

KAW acknowledges summer support under the ASEE visiting faculty program, ARB and MEI acknowledge support from the Office of Naval Research (Physics Div.), and LG acknowledges a NICOP grant from the Office of Naval research (London). We also acknowledge useful discussions with A.D. Hibbs and thank him, and B. Whitecotton for providing the experimental data of Fig. 4.

## References

- [1] K. Wiesenfeld, F. Moss, *Nature* 373 (1995) 33;  
A. Bulsara, L. Gammaitoni, *Phys. Today* 49 (1996) 39;  
L. Gammaitoni, P. Hänggi, P. Jung, F. Marchesoni, *Rev. Mod. Phys.* 70 (1998) 1.
- [2] A. Hibbs, A. Singsaas, E. Jacobs, A. Bulsara, J. Bekkedahl, F. Moss, *J. Appl. Phys.* 77 (1995) 2582;  
R. Rouse, S. Han, J. Lukens, *Appl. Phys. Lett.* 66 (1995) 108.
- [3] A. Bulsara, M. Inghiosa, L. Gammaitoni, *Phys. Rev. Lett.* 77 (1996) 2162;  
M. Inghiosa, A. Bulsara, L. Gammaitoni, *Phys. Rev. E* 55 (1997) 4049;  
M. Inghiosa, A. Bulsara, *Phys. Rev. E* 78 (1998) 115.
- [4] M. Inghiosa, A. Bulsara, A. Hibbs, B. Whitecotton, *Phys. Rev. Lett.* 80 (1998) 1381.
- [5] A. Hibbs, in: *Applied Nonlinear Dynamics and Stochastic Systems Near the Millennium*, AIP Conf. Proc. 411, eds. J. Kadtko, A. Bulsara (AIP Press, New York, 1997);  
A. Hibbs, B. Whitecotton, in: *Proc. of the Applied Superconducting Electronics Conference*, Berlin 1997.
- [6] M. Inghiosa, A. Bulsara, *Phys. Rev. E* 53 (1995) R2021;  
M. Stemmler, *Network* 7 (1996) 687;  
A. Bulsara, A. Zador, *Phys. Rev. E* 54 (1996) 2185;  
C. Heneghan, C. Chow, J. Collins, T. Imhof, S. Lowen, M. Teich, *Phys. Rev. E* 54 (1996) R2228;  
A. Neiman, B. Shulgin, V. Anischenko, L. Schimansky-Geier, J. Freund, *Phys. Rev. Lett.* 76 (1996) 4299;  
F. Chapeau-Blondeau, *Phys. Rev. E* 55 (1997) 2016;  
M. Inghiosa, A. Bulsara, *Phys. Rev. E* 58 (1998) 115;  
V. Galdi, V. Pierro, I. Pinto, *Phys. Rev. E* 57 (1998) 6470;  
J. Robinson, D. Asraf, A. Bulsara, M. Inghiosa, *Phys. Rev. Lett.* 81 (1998).
- [7] A. Barone, G. Paterno, *Physics and Applications of the Josephson Effect* (Wiley, New York, 1982).
- [8] A. de Waele, R. de Bruyn Ouboter, *Physica* 41 (1969) 225;  
A. Matsinger, R. de Bruyn Ouboter, H. van Beelen, *Physica B* 94 (1978) 91;  
C. Tesche, *J. Low Temp. Phys.* 44 (1981) 119;  
E. Ben-Jacob, D. Bergman, Y. Imry, B. Matkowsky, Z. Schuss, *J. Appl. Phys.* 54 (1983) 6533;  
T. Ryhanen, H. Seppä, R. Ilmoniemi, J. Knuutila, *J. Low Temp. Phys.* 76 (1989) 287.
- [9] E. Ben-Jacob, Y. Imry, *J. Appl. Phys.* 52 (1981) 6806;  
P. Carelli, G. Paterno, in: *Principles and Applications of Superconducting Quantum Interference Devices*, ed. A. Barone (World Scientific, Singapore, 1992).